

Scalable Synthesis of Minimum-Information Linear-Gaussian Control by Distributed Optimization

Murat Cubuktepe, Takashi Tanaka, and Ufuk Topcu

Abstract—We consider a discrete-time linear-quadratic Gaussian control problem in which we minimize a weighted sum of the directed information from the state of the system to the control input and the control cost. The optimal control and sensing policies can be synthesized jointly by solving a semidefinite programming problem. However, the existing solutions typically scale cubic with the horizon length. We leverage the structure in the problem to develop a distributed algorithm that decomposes the synthesis problem into a set of smaller problems, one for each time step. We prove that the algorithm runs in time linear in the horizon length. As an application of the algorithm, we consider a path-planning problem in a state space with obstacles under the presence of stochastic disturbances. The algorithm computes a locally optimal solution that jointly minimizes the perception and control cost while ensuring the safety of the path. The numerical examples show that the algorithm can scale to thousands of horizon length and compute locally optimal solutions.

I. INTRODUCTION

We revisit the problem of minimum-information control of linear-Gaussian systems [1]–[7], where the trade-off between the best achievable control performance and the required sensor data rate is studied. Such a trade-off is relevant to the utility-privacy trade-off in multi-party control systems [8]–[11]. It also plays a crucial role in the network control systems design [11]–[13].

The work most related to this paper is [6], where the authors formulated the minimum-information linear-Gaussian control problem as a sensor-controller joint design problem. They showed that the optimal controller can be obtained as the solution to Riccati equations, while the optimal sensor is obtained as the solution to the so-called Gaussian sequential rate-distortion (SRD) problem [5], [14]. They further showed that the Gaussian SRD problem can be formulated as a semidefinite programming problem (SDP), which can be solved by interior-point methods in polynomial time [15], [16]. However, the computation typically requires $\mathcal{O}(T^3)$ time with horizon length T if the structure of the SDP is not exploited, and an interior-point method may not scale to large horizon lengths.

Our first contribution in this work is to exploit the structure of the Gaussian SRD problem to derive a distributed algorithm, which facilitates the sensor design for a large horizon length. We propose a distributed algorithm based on ADMM [17]–[21], which allows us to design sensors on problems with large horizon length. The structure in the problem enables us to develop a distributed algorithm that, given a linear time-varying

dynamical system and data rate constraints, decomposes the original SDP problem to smaller SDP problems, one for each time step. The algorithm then solves the smaller SDP problems in parallel at each iteration. We prove that our algorithm runs in time linear with the horizon length.

Our second contribution is to apply our algorithm to the minimum-sensing path-planning problem, which incorporates the perception cost into a path-planning problem [22]–[27]. A path-planning problem with a similar spirit has been recently considered in [28]. Conventionally, path planning is performed by a global path search (via grid-based algorithms such as A* [29] and randomized algorithms such as RRT [23], [30]), followed by path-smoothing and feedback control design for path following. In this paper, we provide a path-smoothing algorithm that refines a given initial trajectory by computing a locally optimal solution. Our algorithm is closely related to the convex-concave procedure [31], which iteratively finds a locally optimal solution to a difference of convex (DC) problem and to [28], which optimizes a similar metric to our case in a path-planning problem using an RRT*-based method. We formulate the path-smoothing problem with perception cost as a DC problem. Our formulation is convex, except the task constraints, which is to avoid colliding with obstacles. We express the task constraints as reverse convex constraints, which can be used in a DC problem, and a locally optimal solution can be computed.

We show the effectiveness of the algorithms in two numerical examples. To demonstrate our first contribution, we consider attitude determination for a spin-stabilized satellite example. We compute the minimum required information in order to satisfy the required distortion constraints with a substantial horizon length. To demonstrate the second contribution, we solve a path-smoothing problem with multiple obstacles in a two-dimensional state space. The objective is to find a path that is feasible and minimizes the required joint control and perception cost. We show that we can find a locally optimal path within a few iterations.

Organization: Section II introduces the Gaussian SRD problem and the semidefinite programming formulation for the linear-Gaussian sensor design problem. We propose a distributed algorithm based on ADMM in Section III that solves the linear-Gaussian sensor design problem in linear time with the horizon length. We discuss the convergence rate of the algorithm and improvements over the standard ADMM. Section IV provides the application of our algorithm in a path-planning problem. Section V provides two examples to show the validity of our proposed algorithm. Section VI concludes the paper and discusses future directions.

Murat Cubuktepe, Takashi Tanaka, and Ufuk Topcu are with the Department of Aerospace Engineering and Engineering Mechanics, University of Texas, Austin, 201 E 24th St, Austin, TX 78712. email: {mcubuktepe, ttanaka, utopcu}@utexas.edu

II. PROBLEM FORMULATION AND PRELIMINARIES

Notation. We denote vector-valued variables at time step t by $x_t \in \mathbb{R}^n$. $x(T)$ is the collection of all $x_0 \dots x_T$. $A \succ 0$ ($\succeq 0$) denotes that the matrix $A \in \mathbb{R}^{n \times n}$ is positive definite (positive semidefinite). We denote a Gaussian distribution with mean μ and covariance Σ by $\mathcal{N}(\mu, \Sigma)$. The log-determinant of a positive definite matrix A is given by $\log \det A$ and the trace of a matrix A is given by $\text{Tr}(A)$. For a positive semidefinite matrix A , we define $\|x\|_A = \sqrt{x^\top A x}$.

A. Minimum-Information Linear-Gaussian Control

The model that we consider in this paper is the following linear time-varying system

$$x_{t+1} = A_t x_t + B_t u_t + w_t, \quad t = 1, 2, \dots, T-1, \quad (1)$$

where $x_0 \in \mathbb{R}^n \sim \mathcal{N}(0, P_0)$, $P_0 \in \mathbb{R}^{n \times n} \succ 0$ and $w_t \in \mathbb{R}^n \sim \mathcal{N}(0, W_t)$, $W_t \in \mathbb{R}^{n \times n} \succ 0$, $t = 1, 2, \dots, T$ are mutually independent Gaussian random variables, $u_t \in \mathbb{R}^m$, $t = 1, 2, \dots, T-1$ are the control inputs, and $A_t \in \mathbb{R}^{n \times n}$, $B_t \in \mathbb{R}^{n \times m}$, $t = 1, 2, \dots, T-1$ define the dynamics.

The minimum-information linear-Gaussian control problem is formulated as

$$\text{minimize} \quad I(x(T) \rightarrow u(T)) \quad (2)$$

$$\text{subject to} \quad \mathbb{E}\|x_t\|^2 + \|u_t\|^2 \leq \gamma_t, \quad (3)$$

where the minimization is over the causal policies (stochastic kernels) of the form $\{p(u_t|x(t), u(t-1))\}_{t=1,2,\dots,T}$. Positive constants γ_t , $t = 1, 2, \dots, T$ specify user-defined requirements on instantaneous control costs, and the term $I(x(T) \rightarrow u(T))$ is known as *directed information* [32]:

$$I(x(T) \rightarrow u(T)) \triangleq \sum_{t=1}^T I(x(t); u_t | u(t-1)), \quad (4)$$

where $I(x(t); u_t | u(t-1))$ is the conditional mutual information. It can be shown [5] that the optimal policy for (2)-(3) can be realized by a three-stage structure comprised of

- (i) a linear sensor mechanism

$$y_t = C_t x_t + v_t, \quad t = 1, 2, \dots, T, \quad (5)$$

where $v_t \sim \mathcal{N}(0, V_t)$, $V_t \succ 0$ are mutually independent Gaussian random variables;

- (ii) the least mean square error estimator (Kalman filter)

$$z_t = \mathbb{E}(x_t | y(t)), \quad t = 1, 2, \dots, T; \text{ and} \quad (6)$$

- (iii) the certainty equivalence controller $u_t = K_t z_t$.

Observing that the optimal control gain K_t in (iii) can be pre-calculated by solving a backward Riccati equation, the problem (2)–(3) can be reduced to the optimal sensor design problem [5]

$$\text{minimize} \quad I(x(T) \rightarrow z(T)) \quad (7)$$

$$\text{subject to} \quad \mathbb{E}\|x_t - z_t\|_{\Theta_t}^2 \leq \gamma_t - c_t (:= D_t), \quad (8)$$

where the minimization is over the sensor mechanism (5) (decision variables are matrices C_t and V_t) and z_t is computed by (6). Constants $\Theta_t \succ 0$ and c_t are obtained from the solution

to the aforementioned backward Riccati equation. The problem (7)–(8) is known as the Gaussian sequential rate-distortion (SRD) problem [33] (also known as the nonanticipative rate-distortion problem [14]).

B. SDP Formulation of the Gaussian SRD Problem

It can be further shown (see [6] for the derivation) that the Gaussian SRD problem (7)–(8) can be written as a SDP

$$\text{minimize} \quad - \sum_{t=1}^T \log \det \Pi_t \quad (9)$$

$$\text{subject to} \quad P_{T|T} = \Pi_T, \Pi_t \succ 0, \quad t = 1, 2, \dots, T, \quad (10)$$

$$\begin{bmatrix} P_{t|t} - \Pi_t & P_{t|t} A_t^\top \\ A_t P_{t|t} & W_t + A_t P_{t|t} A_t^\top \end{bmatrix} \succeq 0, \quad t = 1, 2, \dots, T-1, \quad (11)$$

$$\text{Tr}(\Theta_t P_{t|t}) \leq D_t, \quad t = 1, 2, \dots, T-1, \quad (12)$$

$$P_{t+1|t+1} \preceq A_t P_{t|t} A_t^\top + W_t, \quad t = 1, 2, \dots, T-1, \quad (13)$$

where $P_{t|t}, \Pi_t \in \mathbb{R}^{n \times n}$ are the problem variables, and A_t, W_t, D_t, Θ_t are given problem data. Once the optimal solution $\{P_{t|t}\}_{t=1,2,\dots,T}$ to (9)–(13) is obtained, the optimal sensor mechanism (5) can be obtained by choosing the matrices C_t and V_t to satisfy

$$P_{t|t}^{-1} - (A_{t-1} P_{t-1|t-1} A_{t-1}^\top + W_{t-1})^{-1} = C_t^\top V_t^{-1} C_t.$$

C. Problem Statement

Reference [5] notes that solving the SDP (9)–(13) typically requires $\mathcal{O}(T^3)$ time. However, that generally holds if there is no sparsity pattern in the SDP problem that can be exploited. We note that the only coupling constraints between different time-steps in the SDP (9)–(13) is the constraint in (13), and we propose a method to decouple these constraints for different time-steps, which facilitates solving the linear-Gaussian sensor design problem in $\mathcal{O}(T)$ time. Specifically, we solve the following problem.

Problem 1. *Given the dynamics A_t , the Gaussian noise matrices W_t , and coefficients D_t for $t = 1, \dots, T$, derive an algorithm that solves the SDP (9)–(13) in $\mathcal{O}(T)$ time.*

In addition to solving Problem 1 in Section III, we also discuss how we utilize our methods for the Gaussian SRD problem to a path-planning problem in Section IV.

III. DISTRIBUTED SENSOR DESIGN USING ADMM

In this section, we derive our distributed algorithm for the linear-Gaussian sensor design problem. We introduce alternating direction method of multipliers (ADMM) [17], which is frequently used in distributed optimization. We then derive our formulation to decouple the constraints in (13) for different time steps. We prove that by construction, our algorithm also runs in time linear with the horizon length T .

A. ADMM

ADMM can be used to solve the following constrained optimization problem

$$\text{minimize} \quad f(j)$$

$$\text{subject to} \quad j \in \mathcal{C},$$

where $j \in \mathbb{R}^n$ is the problem variable, f and \mathcal{C} are convex. We rewrite the problem in ADMM form as

$$\begin{aligned} & \text{minimize} && f(j) + g(k) \\ & \text{subject to} && j = k, \end{aligned}$$

where g is the indicator function of \mathcal{C} .

The augmented Lagrangian with the scaled dual variable $l \in \mathbb{R}^n$ for this problem is

$$L_\rho(j, k, l) = f(j) + g(k) + (\rho/2)\|j - k + l\|_2^2,$$

which is obtained by combining the terms in the augmented Lagrangian, see [17, Section 3.1.1] for details. The ADMM iterations for this problem are

$$\begin{aligned} j^{m+1} &:= \operatorname{argmin}\{f(j) + (\rho/2)\|j - k^m - l^m\|_2^2\}, \\ k^{m+1} &:= \pi_{\mathcal{C}}(j^{m+1} + k^m), \\ l^{m+1} &:= l^m + j^{m+1} - k^{m+1}, \end{aligned}$$

where $\rho \in \mathbb{R}_+$ is a penalty parameter, j^m is the value of j after m 'th iteration and $\pi_{\mathcal{C}}$ denotes projection onto \mathcal{C} .

The j -update involves minimizing f plus a convex quadratic function, i.e., evaluation of the proximal operator associated with f . The k -update is Euclidean projection onto \mathcal{C} .

B. Distributed Linear-Gaussian Sensor Design

We now give our algorithm that solves the linear-Gaussian sensor design problem in $\mathcal{O}(T)$ time. Our algorithm involves constructing an equivalent problem to the problem in (9)–(13) and deriving ADMM updates that can be computed in $\mathcal{O}(T)$ time, which proves that we can solve the Gaussian SRD problem in time linear with the horizon length T .

Theorem 1. *The Gaussian SRD problem can be solved in $\mathcal{O}(T)$ time with the horizon length T .*

Proof. Our proof is based on constructing an equivalent optimization problem that can be solved in a distributed manner with ADMM such that each ADMM update runs in time linear with the horizon length T .

We rewrite the SDP (9)–(13) by adding additional variables K_t , $Q_{t|t}$, and S_t , and the additional constraints in (18)–(19),

$$\text{minimize} \quad - \sum_{t=1}^T \log \det \Pi_t \quad (14)$$

$$\text{subject to} \quad P_{T|T} = \Pi_T, \Pi_t \succ 0, \quad t = 1, 2, \dots, T, \quad (15)$$

$$\begin{bmatrix} P_{t|t} - \Pi_t & P_{t|t} A_t^\top \\ A_t P_{t|t} & W_t + A_t P_{t|t} A_t^\top \end{bmatrix} \succeq 0, \quad t = 1, 2, \dots, T-1, \quad (16)$$

$$\operatorname{Tr}(\Theta_t P_{t|t}) \leq D_t, \quad t = 1, 2, \dots, T-1, \quad (17)$$

$$P_{t+1|t+1} + S_t = A_t Q_{t|t} A_t^\top + W_t, \quad t = 1, 2, \dots, T-1, \quad (18)$$

$$K_t \succeq 0, \quad Q_{t|t} = P_{t|t}, \quad S_t = K_t, \quad t = 1, 2, \dots, T-1. \quad (19)$$

By construction, it is clear that the optimization problem in (9)–(13) shares the same objective value and set of optimal solutions with the problem (14)–(19).

We rewrite the above problem in ADMM form with j denoting the variables for S_t and $Q_{t|t}$, k denoting the variables for $P_{t|t}$, Π_t , K_t , and $f(j)$ is the indicator function for (18)

and $g(k)$ is the sum of the objective in (14) and the indicator functions for (15)–(17) and $K_t \succeq 0$.

We now construct the ADMM iterations as follows. The j -update is given by solving the following convex problem

$$\begin{aligned} & \text{minimize} && \sum_{t=1}^{T-1} (\|Q_{t|t} - P_t^m + U_t^m\|_F^2 + \\ & && \|S_t - K_t^m + V_t^m\|_F^2) \end{aligned}$$

subject to

$$P_{t+1|t+1} + S_t = A_t Q_{t|t} A_t^\top + W_t, \quad t = 1, 2, \dots, T-1,$$

with variables $Q_{t|t}$ and S_t . U_t denotes the dual variable for the constraint $Q_{t|t} = P_{t|t}$ and V_t denotes the dual variable for the constraint $S_t = K_t$, and $\|\cdot\|_F$ denotes the Frobenius norm of a matrix. This problem is separable with each time step $t = 1, 2, \dots, T$, meaning that the optimal solution can be obtained by solving for each time step t separately. Therefore, j -update can be done in time linear in T .

Let $\{Q_{t|t}^{m+1}, K_t^{m+1}\}_{t=1,2,\dots,T-1}$ be the optimal solution of this convex optimization problem. Then, the k -update is given by solving the following SDP

$$\text{minimize} \quad - (2/\rho) \sum_{t=1}^T \log \det \Pi_t +$$

$$\sum_{t=1}^{T-1} (\|Q_{t|t}^{m+1} - P_t + U_t^m\|_F^2 + \|S_t^{m+1} - K_t + V_t^m\|_F^2)$$

$$\text{subject to} \quad P_{T|T} = \Pi_T, \Pi_t \succ 0, \quad t = 1, 2, \dots, T-1,$$

$$\begin{bmatrix} P_{t|t} - \Pi_t & P_{t|t} A_t^\top \\ A_t P_{t|t} & W_t + A_t P_{t|t} A_t^\top \end{bmatrix} \succeq 0, \quad t = 1, 2, \dots, T-1,$$

$$\operatorname{Tr}(\Theta_t P_{t|t}) \leq D_t, \quad K_t \succeq 0, \quad t = 1, 2, \dots, T-1,$$

with variables Π_t , $P_{t|t}$ and K_t for $t = 1, 2, \dots, T$. Note that this problem also is separable with each time step t .

Let $\{\Pi_t^{m+1}, P_t^{m+1}, K_t^{m+1}\}_{t=1,2,\dots,T}$ be the optimal solution of this SDP. Then, the l -update is given by

$$U_t^{m+1} = U_t^k + Q_{t|t}^{m+1} - P_t^{m+1},$$

$$V_t^{m+1} = V_t^m + K_t^{m+1} - S_t^{m+1},$$

for $t = 1, 2, \dots, T-1$. The dual update also scales linearly with T . This completes our proof. \square

Our algorithm solves the linear-Gaussian sensor design problem, which is the most computationally challenging part of solving the minimum-information linear-quadratic Gaussian problem in time linear with horizon length. In the following, we discuss the convergence rate of the algorithm and how we can improve the convergence rate of ADMM.

C. Improvements over the Standard ADMM

ADMM can generate solutions with moderate accuracy after the first few tens of iterations and solve large-scale problems effectively [17]. However, ADMM can be very slow to converge to a highly accurate solution. In this section, we discuss some theoretical properties of the proposed algorithm and possible improvements to improve the convergence rate.

1) *Convergence Rate of the Algorithm:* ADMM can achieve linear convergence rate, i.e., requiring $\mathcal{O}(\log(1/\epsilon))$ iterations to achieve ϵ accuracy by choosing a small enough step-size in the dual update [20], or if f is strongly convex [34].

2) *Using Acceleration Steps:* An extension to ADMM is to use an additional acceleration step, which is including additional update steps in the k -update and the dual update. It is empirically shown in [35] that acceleration steps can significantly improve the convergence rate. Adding an acceleration step requires the objective f to be strongly convex to ensure convergence. Therefore, additional strongly convex terms are required to be added to the objective in the j -update, such as $\mu (\|Q_{t|t}\|_F^2 + \|S_t\|_F^2)$, where μ is a positive parameter.

The acceleration step is carried out by modifying the ADMM iterations as

$$\begin{aligned} j^{m+1} &:= \operatorname{argmin}\{f(j) + (\rho/2)\|j - \hat{k}^m + \hat{l}^m\|_2^2\}, \\ k^{m+1} &:= \pi_C(j^{m+1} + \hat{l}^m), \\ l^m &:= \hat{l}^m + \rho(j^{m+1} - k^{m+1}), \\ \beta^{m+1} &:= (1 + \sqrt{1 + 4\beta^m})/2, \\ \hat{k}^{m+1} &:= k^m + \frac{\beta^m - 1}{\beta^{m+1}}(k^m - k^{m-1}), \\ \hat{l}^{m+1} &:= l^m + \frac{\beta^m - 1}{\beta^{m+1}}(l^m - l^{m-1}), \end{aligned}$$

where β^m is the acceleration parameter, and $\beta^0 = 0$. Restarting the algorithm here refers to setting the acceleration parameter to 0 during the iterations.

3) *Over-relaxation:* Over-relaxation is done by replacing j^{m+1} with $\gamma^m j^{m+1} - (1 - \gamma^m)j^m$ in k - and l -updates. $\gamma^m \in (0, 2)$ is a relaxation parameter. When $\gamma^m > 1$, this technique is called over-relaxation, and when $\gamma^m < 1$, it is called under-relaxation. The intuition in over-relaxation is to take an additional step in the k - and l -updates. References [36], [37] analyze the convergence of over-relaxation for different parameters. Experiments in [38], [39] suggest that over-relaxation with $\gamma^m \in [1.5, 1.8]$ can improve convergence.

IV. APPLICATIONS TO PATH-PLANNING PROBLEM

In this section, we leverage our SDP-based formulation to synthesize an optimal control and sensing policy to the path-smoothing problem. The path-smoothing problem we consider has a similar structure to (9)–(13) with additional variables and constraints. The ADMM-based algorithms provided in the previous section are largely applicable. We provide an algorithm for the path-smoothing problem that locally optimizes a weighted sum of the control and perception cost from any given trajectory by iteratively convexifying the problem around the trajectory. Our algorithm computes a locally optimal solution, and if the given trajectory is feasible, then all successive trajectories are guaranteed to be feasible.

Suppose (1) represents the dynamics of a mobile robot under stochastic disturbances, where $x_t \in \mathbb{R}^n$ for $t = 1, 2, \dots, T$ is the position of the robot, and $u_t \in \mathbb{R}^m$ for $t = 1, 2, \dots, T-1$ is the control input. Let $X_{\text{obs}} \in \mathbb{R}^n$ be a closed set of points

that represents the obstacles to avoid. We can formulate the path-planning problem by modifying the objective in (9) by

$$\text{minimize } \sum_{t=1}^T (-\log \det \Pi_t + (1/\alpha)\|u_t\|_2^2) \quad (20)$$

and adding the following constraints to (10)–(13),

$$u_t \in \mathcal{U}_t, \quad t = 1, 2, \dots, T-1, \quad (21)$$

$$x_t \in \mathcal{X}_t, \quad t = 1, 2, \dots, T, \quad (22)$$

$$x_{t+1} = A_t x_t + B_t u_t, \quad t = 1, 2, \dots, T-1, \quad (23)$$

$$(x_t - x_{\text{obs}})^\top P_{t|t}^{-1} (x_t - x_{\text{obs}}) \geq \chi^2, \quad (24)$$

$$t = 1, 2, \dots, T, \quad \forall x_{\text{obs}} \in X_{\text{obs}},$$

where $\alpha \in \mathbb{R}_+$ is a parameter that gives the trade-off between the control and the perception cost, $\chi^2 \in \mathbb{R}_+$ is a confidence level parameter, $A_t \in \mathbb{R}^{n \times n}$ and $B_t \in \mathbb{R}^{n \times m}$ are given matrices, and $x_{\text{obs}} \in \mathbb{R}^n$ are the obstacles. Here, we are adopting the notion of path-planning in the so-called *uncertain configuration space* [40], i.e., designing the sequence of mean x_t and covariance $P_{t|t}$ jointly.

The objective in (20) minimizes a trade-off between the perception and control cost. The constraints in (21)–(22) represent the constraints in the inputs and final state. The constraints in (23) give the dynamics of the linear time-varying process, and (24) ensures that the uncertainty ellipsoid given by $P_{t|t}$ around the trajectory x_t does not intersect with the obstacles. The problem in (10)–(13) and (20)–(24) is a convex optimization problem without the constraints in (24), which is a nonconvex constraint in general.

Remark 1. We can include any convex cost, such as in the position or control variables in the objective (20). In this paper, we consider control and perception cost for simplicity.

We use the penalty convex-concave procedure (CCP) [31], which iteratively over-approximates a non-convex optimization problem via linearization. The resulting convex problem can then be solved efficiently, and we iterate the process until we compute a locally optimal solution. Specifically, we compute affine upper bounds for the convex functions in (21). CCP improves the solution by convexifying the problem around the previous solution iteratively.

To perform CCP, we start with any initial trajectory $\{\hat{x}_t, \hat{P}_{t|t}\}_{t=1,2,\dots,T}$ in the uncertain configuration space and convexify the constraints in (24) for $t = 1, 2, \dots, T, \quad \forall x_{\text{obs}} \in X_{\text{obs}}$ as

$$\begin{aligned} x_{t,\text{obs}} &= (x_t - x_{\text{obs}}), \\ h(x_t, P_{t|t}, x_{\text{obs}}) &= x_{t,\text{obs}}^\top P_{t|t}^{-1} x_{t,\text{obs}}, \\ \bar{h}(x_t, P_{t|t}, x_{\text{obs}}) &= h(\hat{x}_t, \hat{P}_{t|t}, x_{\text{obs}}) + \end{aligned} \quad (25)$$

$$\begin{aligned} \nabla h(\hat{x}_t, \hat{P}_{t|t}, x_{\text{obs}}) &(\hat{x}_t - x_t, \hat{P}_{t|t} - P_{t|t}, x_{\text{obs}}), \\ \nabla h(\hat{x}_t, \hat{P}_{t|t}, x_{\text{obs}}) &= -\hat{P}_{t|t}^{-1} x_{t,\text{obs}} x_{t,\text{obs}}^\top \hat{P}_{t|t}^{-1}, \end{aligned} \quad (26)$$

$$\bar{h}(x_t, P_{t|t}, x_{\text{obs}}) \geq \chi^2, \quad (27)$$

where (25) computes an affine approximation of the convex function h around $(\hat{x}_t, \hat{P}_{t|t})$ and (26) is the gradient of h at $(\hat{x}_t, \hat{P}_{t|t})$. (27) is the resulting convexified constraint.

The function \bar{h} is a *convex over-approximation* of the original function h as we compute an affine lower bound of h . As a direct consequence, any feasible assignment for the resulting over-approximated and convex problem is also feasible for the original nonconvex problem. However, the resulting convex problem might be infeasible, even though the original problem is not. To find a feasible assignment, we assign a non-negative penalty variable $m_{t,\text{obs}}$ for each of the convexified constraints by modifying the constraint (27) as

$$m_{t,\text{obs}} + \bar{h}(x_t, P_{t|t}, x_{\text{obs}}) \geq \chi^2 \quad (28)$$

to ensure that the convexified problem is always feasible [31, Section 3.1]. To find a solution that minimizes violations to the convexified constraints, we minimize the sum of the penalty variables. We then solve the convex problem with the objective

$$\begin{aligned} \text{minimize} \quad & \sum_{t=1}^T (-\log \det \Pi_t + (1/\alpha) \|u_t\|_2^2) + \\ & \tau \sum_{t=1}^T \sum_{x_{\text{obs}} \in X_{\text{obs}}} m_{t,\text{obs}} \end{aligned}$$

and the constraints in (10)–(13), (21)–(23) and (28) where τ is a positive penalty parameter that minimizes a trade-off between the objective and the violations of the constraints. If all penalty variables are assigned to zero, then the solution of the convex problem is feasible for the original non-convex path-planning problem, as we over-approximate the convex functions by affine functions. If any of the penalty variables $m_{t,\text{obs}}$ are assigned to a positive value, we update the penalty parameter τ by $\mu \cdot \tau$ for a $\mu > 0$, similar to [31, Algorithm 3.1].

After getting a new solution, we convexify the non-convex constraints by linearizing the convex functions around the new solution and solve the resulting convex SDP. We repeat the procedure until we find a feasible and locally optimal solution. If the procedure converges to an infeasible solution, we restart the procedure with another initial trajectory. Note that the procedure converges to a locally optimal solution for a fixed τ , i.e., after $\tau = \tau_{\text{max}}$, but it may converge to an infeasible point of the original problem [31, Section 1.3].

Remark 2. *If the initial trajectory is feasible, we can set the penalty variables $m_{t,\text{obs}}$ to zero, and all subsequent trajectories are guaranteed to be feasible after each iteration of the CCP [31].*

V. NUMERICAL EXAMPLES

We evaluate our distributed sensor and control design procedure in two numerical examples. The experiments are performed on a computer with an Intel Core i9-9900u 2.50 GHz processor and 64 GB of RAM with Mosek [41] as the SDP solver. The first example is on computing the minimal information to estimate the attitude of a satellite subject to accuracy constraints. The second example is on a path-smoothing problem in a two-dimensional state space containing multiple obstacles in order to illustrate the effects of varying the trade-offs between the control and perception cost.

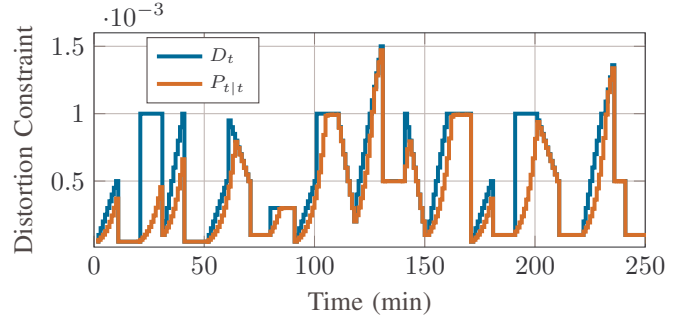


Figure 1: Plot of the time-varying distortion constraint D_t and the traces of the optimal covariance matrices $P_{t|t}$ for the first 250 minutes of the mission.

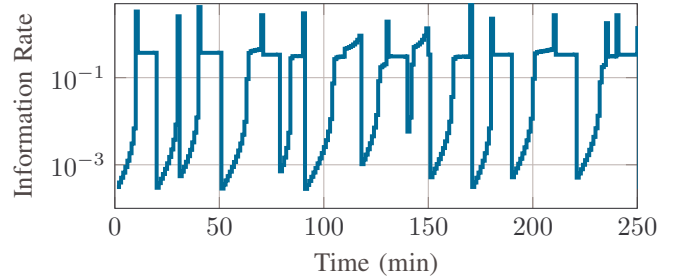


Figure 2: Plot of the optimal information rate $I(x(t) : y_t | y(t-1))$ for the first 250 minutes of the mission.

A. Satellite Attitude Determination

In this example, we consider the spin-stabilized satellite example from [6]. The equation of motion of the angular velocity vector of a spin-stabilized satellite linearized around the nominal angular velocity vector $(\omega_0, 0, 0)$ is

$$\begin{bmatrix} d\omega_1 \\ d\omega_2 \\ d\omega_3 \end{bmatrix} = \begin{bmatrix} 1 & 0 & \frac{I_3 - I_1}{I_2} \omega_0 \\ 0 & 1 & 0 \\ 0 & \frac{I_1 - I_2}{I_3} \omega_0 & 1 \end{bmatrix} \begin{bmatrix} \omega_1 \\ \omega_2 \\ \omega_3 \end{bmatrix} dt + d\mathbf{b}$$

where \mathbf{b} is a disturbance, I_1, I_2 , and I_3 are the moment of inertias in three dimensions. We convert the continuous-time dynamics into a discrete-time model in the experiments. The objective is to figure out the sensing pattern that uses minimal information during the mission. We consider a horizon length $T = 1500$ with the distortion rate constraint given in Figure 1.

We plot the optimal covariance scheduling $P_{t|t}$ and the optimal information rate in Figures 1 and 2 for the first 250 time-steps. We put a log-scale on the y -axis in Figure 2 to emphasize that the optimal covariance scheduling requires some information rate in all time steps, which is not the case in the numerical examples in [6]. The reason that there is a requirement of some information in all time steps may stem from having a less accurate solution from an ADMM-based algorithm rather than from an interior-point method. We can see that the information rate varies significantly during the mission, and the optimal information rate is minimal if the distortion rate constraint is not restrictive.

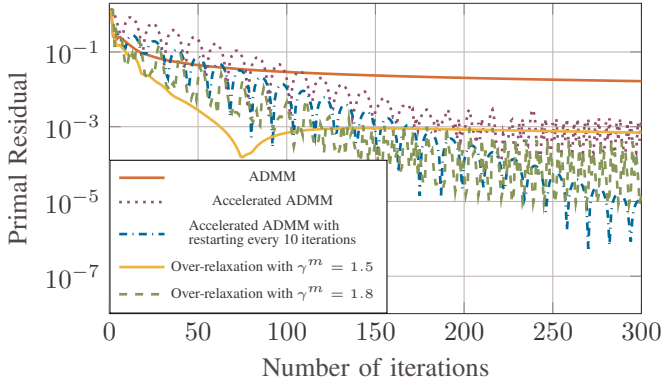


Figure 3: Primal residuals for the spin-stabilized satellite example for standard ADMM, accelerated ADMM, and over-relaxed ADMM with $\rho = 1$. Accelerated ADMM with restart achieves the best performance.

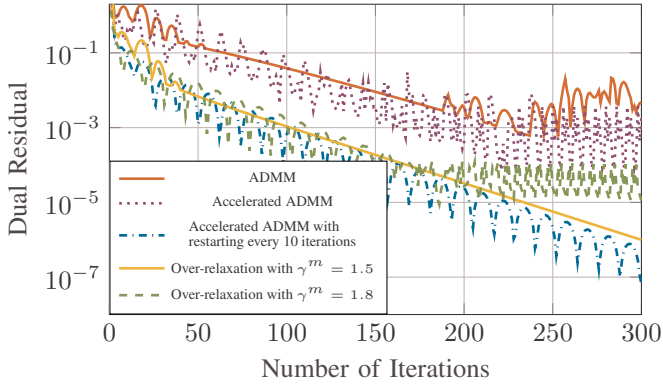


Figure 4: Dual residuals for the spin-stabilized satellite example for standard ADMM, accelerated ADMM, and over-relaxed ADMM with $\rho = 1$. Accelerated ADMM with restart achieves the best performance.

We now show the convergence rate of the ADMM-based algorithms by plotting the norm of the primal residual, which is given by $r_t^1 = P_t - Q_t$ and $r_t^2 = S_t - K_t$ and the dual residual, which is $d_t^1 = \rho(P_t - P_{t-1})$ and $d_t^2 = \rho(K_t - K_{t-1})$ for different methods [17, Section 3.3]. The primal residual denotes the infeasibility of the methods in each iteration, and the dual residual denotes the optimality of the methods. If the primal residual is small, then the variables approach to a feasible solution. If the dual residual is small, then the variables approach to an optimal solution.

We list the convergence rates of the over-relaxation and accelerated variants of the ADMM in Figures 3–4. We plot the primal residuals, in Figure 3 we plot the dual residuals in Figure 4. Residuals for the spin-stabilized satellite example for regular ADMM and over-relaxed ADMM with $\rho = 1$.

We note that the over-relaxation and the accelerated variants of the ADMM achieve higher accuracy than the standard ADMM. However, the tail convergence of the methods can be very slow. Accelerated ADMM with restarting the acceleration parameter in every ten iterations achieves feasibility with higher accuracy compared to other methods, and the tail

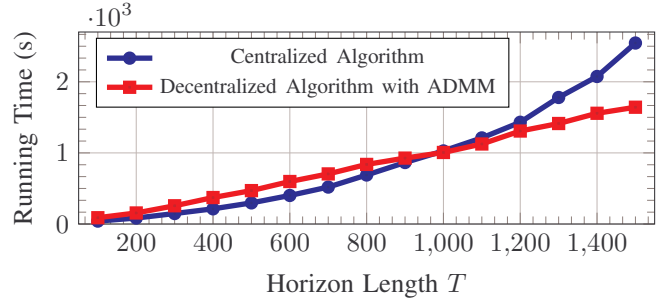


Figure 5: The running times of the distributed and centralized algorithms with a different number of horizon lengths after 50 iterations with the distributed algorithm. The distributed algorithm scales linearly with the number of horizon length. The centralized algorithm is slower than the distributed algorithm with an increasing number of horizon lengths and does not scale linearly.

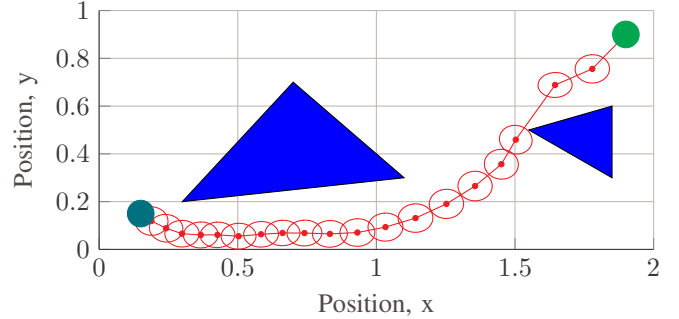


Figure 6: The plot of the initial trajectory with covariance matrices. The small red dots denote the expected state at different time steps, and the red ellipsoids are χ^2 covariance ellipses representing 90% certainty regions. The blue regions and the boundaries are the obstacles to avoid.

convergence is faster compared to the other methods.

For dual residuals, both of the over-relaxation schemes achieve better accuracy. However, the iterates change very slowly before a high accuracy in the primal residual is achieved, which is not a desired property. On the other hand, accelerated ADMM with restarting the acceleration parameter in every ten iterations achieves very high accuracy in the dual residual, and the resulting solution has very high accuracy.

We show the running time of the distributed and the centralized algorithm, which is solving the SDP in (9)–(13) directly, for the different number of horizon lengths in Figure 5. The results in Figure 5 show that the running time of the distributed algorithm scales linearly with the horizon length and is faster than the centralized algorithm with a higher horizon length.

B. Path Planning with Multiple Obstacles

We consider a path-planning problem with multiple obstacles in a two-dimensional state space. We consider an example with $\alpha = 10, 1, 0.1, 0.001$ to illustrate the effects of varying the trade-offs between the perception and control cost.

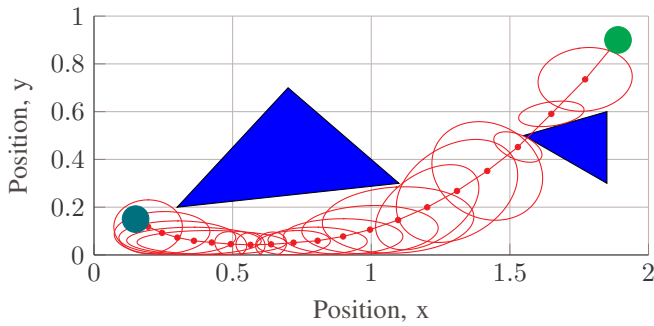


Figure 7: Resulting trajectory after 50 CCP iterations with $\alpha = 0.1$. The expected values of the locations at each time step are feasible. However, the trajectory may collide with the obstacles as the direct path between the locations in different time-steps crosses one of the obstacles.

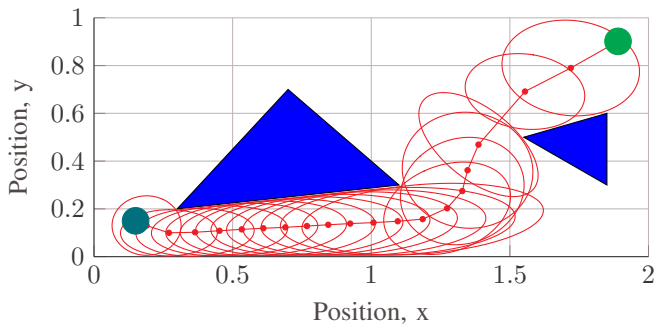


Figure 8: Resulting trajectory after 50 CCP iterations with $\alpha = 10$. The procedure maximizes the distance between the obstacles and the trajectory by minimizing the perception cost.

We plot the initial trajectories in Figure 6, where the red dots represent the expected position vector x_t at time step t and the red χ^2 covariance ellipsoids represent 90% certainty regions. Larger covariance ellipsoids indicate a lower perception cost. We depict the initial and final points with teal and green dots. We consider the boundaries as obstacles. The initial trajectory requires a very high perception cost as the covariance matrices around the trajectory is small in magnitude. In this example, we consider $W_t = 10^{-2}I$ for all time-steps t .

The resulting trajectories after 50 CCP iterations are shown in Figures 7 and 8. The trajectories are feasible, and also has a much larger uncertainty around the waypoints, which minimizes the perception cost. However, the shortest path between the points of the trajectory with $\alpha = 0.01$ is infeasible as it crosses the obstacles, and the resulting trajectory may be infeasible in practice with a higher probability than the one with $\alpha = 1$. We also demonstrate both of the trajectories in the video¹ to demonstrate the trade-offs of having different perception costs on a ground robot. The robot can follow the trajectory with $\alpha = 1$ safely, whereas the trajectory with $\alpha = 0.01$ results in the robot colliding with the obstacle.

To assess the robustness of the trajectories, we run a-

¹<https://bit.ly/2UvCi26>

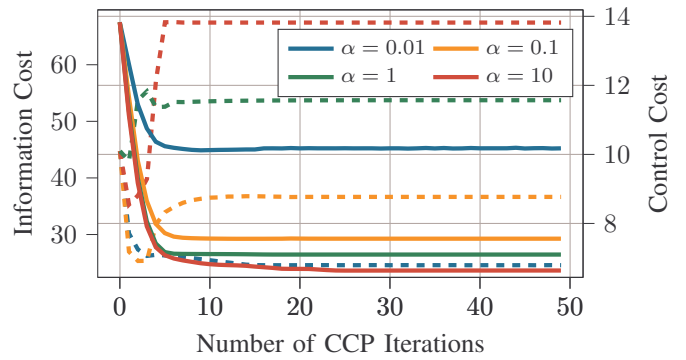


Figure 9: Perception and control costs versus the number of iterations with different values of α . The iterates converge to a locally optimal solution with different parameters, and the resulting perception cost is lower with a higher value of α .

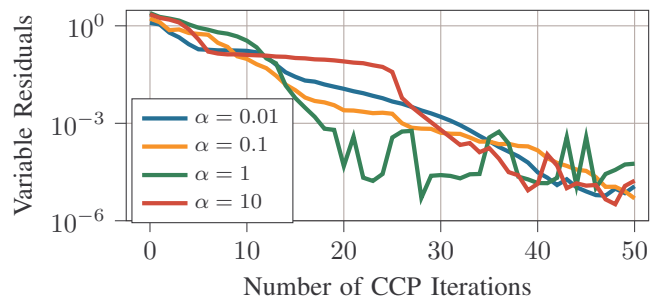


Figure 10: Convergence rate of the procedure with different values of α . All problems converge to a solution within an accuracy of 10^{-4} after 50 CCP iterations.

posteriori Monte-Carlo analysis with different trade-offs of perception cost. We perturb each element of the matrix A_t with $N = 10^6$ samples drawn from a zero-mean uniform distribution with an interval length of 10^{-2} . If we apply the exact inputs that we obtained with $\alpha = 0.01$ on the perturbed dynamics, the estimated probability of resulting path being infeasible is 0.2827, even though the nominal trajectory is feasible. On the other hand, if we apply the inputs with $\alpha = 1$ on the same perturbed dynamics, the estimated probability of an infeasible path is 0.0234, which results in a nominal trajectory that is more robust to the modeling errors.

The resulting perception and control costs with different trade-offs are shown in Figure 9. The solid lines depict the perception costs, and the dashed lines depict the control costs. We observe that with all different trade-offs of the perception and control costs, the methods converge to a locally optimal solution within a few tens of iterations. As expected, the resulting perception costs decrease, and the control cost increase with an increasing value of α . We also plot the convergence rate with different values of α in Figure 10, where x -axis shows the difference between the obtained state values x and covariance values P to the converged solution at each iteration, and the slopes of the figures indicate the rate of convergence. All problems with different values of α converge to a solution within an accuracy of 10^{-4} after 50 iterations.

VI. CONCLUSIONS AND FUTURE WORK

We developed a distributed algorithm for solving the minimum-information linear-Gaussian control problem and applied the algorithm to the minimum-sensing path-planning problem. Our algorithm can scale to very large horizon lengths and runs in time linear with the horizon length. Future work involves establishing the optimal convergence rate given the problem data and determining the optimal parameter selection in different ADMM methods to achieve a faster convergence rate. We will also consider nonlinear and multi-agent systems, and integrate our approach to sampling-based methods for path-planning problems.

REFERENCES

- [1] V. S. Borkar and S. K. Mitter, "LQG Control with Communication Constraints," in *Communications, Computation, Control, and Signal Processing*, pp. 365–373, Springer, 1997.
- [2] S. Tatikonda, A. Sahai, and S. Mitter, "Stochastic Linear Control over a Communication Channel," *IEEE transactions on Automatic Control*, vol. 49, no. 9, pp. 1549–1561, 2004.
- [3] E. I. Silva, M. S. Derpich, J. Østergaard, and M. A. Encina, "A Characterization of the Minimal Average Data Rate that Guarantees a Given Closed-Loop Performance Level," *IEEE Transactions on Automatic Control*, vol. 61, no. 8, pp. 2171–2186, 2015.
- [4] S. Yüksel, "Jointly Optimal LQG Quantization and Control Policies for Multi-Dimensional Systems," *IEEE Transactions on Automatic Control*, vol. 59, no. 6, pp. 1612–1617, 2013.
- [5] T. Tanaka, P. M. Eshfahani, and S. K. Mitter, "LQG Control with Minimum Directed Information: Semidefinite Programming Approach," *IEEE Transactions on Automatic Control*, vol. 63, no. 1, pp. 37–52, 2017.
- [6] T. Tanaka, K.-K. K. Kim, P. A. Parrilo, and S. K. Mitter, "Semidefinite Programming Approach to Gaussian Sequential Rate-Distortion Tradeoffs," *IEEE Transactions on Automatic Control*, vol. 62, no. 4, pp. 1896–1910, 2017.
- [7] V. Kostina and B. Hassibi, "Rate-Cost Tradeoffs in Control," *IEEE Transactions on Automatic Control*, vol. 64, no. 11, pp. 4525–4540, 2019.
- [8] Z. Huang, S. Mitra, and G. Dullerud, "Differentially Private Iterative Synchronous Consensus," in *Proceedings of the 2012 ACM workshop on Privacy in the electronic society*, pp. 81–90, 2012.
- [9] N. E. Maniara and C. N. Hadjicostis, "Privacy-Preserving Asymptotic Average Consensus," in *2013 European Control Conference (ECC)*, pp. 760–765, IEEE, 2013.
- [10] Y. Mo and R. M. Murray, "Privacy Preserving Average Consensus," *IEEE Transactions on Automatic Control*, vol. 62, no. 2, pp. 753–765, 2016.
- [11] Y. Wang, Z. Huang, S. Mitra, and G. E. Dullerud, "Entropy-Minimizing Mechanism for Differential Privacy of Discrete-Time Linear Feedback Systems," in *53rd IEEE conference on decision and control*, pp. 2130–2135, IEEE, 2014.
- [12] Y. Wang, Z. Huang, S. Mitra, and G. E. Dullerud, "Differential Privacy in Linear Distributed Control Systems: Entropy Minimizing Mechanisms and Performance Tradeoffs," *IEEE Transactions on Control of Network Systems*, vol. 4, no. 1, pp. 118–130, 2017.
- [13] J. Cortés, G. E. Dullerud, S. Han, J. Le Ny, S. Mitra, and G. J. Pappas, "Differential Privacy in Control and Network Systems," in *2016 IEEE 55th Conference on Decision and Control (CDC)*, pp. 4252–4272, IEEE, 2016.
- [14] P. A. Stavrou, T. Charalambous, C. D. Charalambous, and S. Loyka, "Optimal Estimation via Nonanticipative Rate Distortion Function and Applications to Time-Varying Gauss–Markov Processes," *SIAM Journal on Control and Optimization*, vol. 56, no. 5, pp. 3731–3765, 2018.
- [15] A. Ben-Tal and A. Nemirovski, *Lectures on Modern Convex Optimization: Analysis, Algorithms, and Engineering Applications*, vol. 2. Siam, 2001.
- [16] S. Boyd, S. P. Boyd, and L. Vandenberghe, *Convex Optimization*. Cambridge university press, 2004.
- [17] S. Boyd, N. Parikh, E. Chu, B. Peleato, J. Eckstein, *et al.*, "Distributed Optimization and Statistical Learning via the Alternating Direction Method of Multipliers," *Foundations and Trends® in Machine learning*, vol. 3, no. 1, pp. 1–122, 2011.
- [18] B. He, H. Yang, and S. Wang, "Alternating Direction Method with Self-Adaptive Penalty Parameters for Monotone Variational Inequalities," *Journal of Optimization Theory and applications*, vol. 106, no. 2, pp. 337–356, 2000.
- [19] S. Wang and L. Liao, "Decomposition Method with a Variable Parameter for a Class of Monotone Variational Inequality Problems," *Journal of optimization theory and applications*, vol. 109, no. 2, pp. 415–429, 2001.
- [20] M. Hong and Z.-Q. Luo, "On the Linear Convergence of the Alternating Direction Method of Multipliers," *Mathematical Programming*, vol. 162, no. 1–2, pp. 165–199, 2017.
- [21] B. O’Donoghue and E. Candes, "Adaptive Restart for Accelerated Gradient Schemes," *Foundations of computational mathematics*, vol. 15, no. 3, pp. 715–732, 2015.
- [22] B. Paden, M. Čáp, S. Z. Yong, D. Yershov, and E. Frazzoli, "A Survey of Motion Planning and Control Techniques for Self-Driving Urban Vehicles," *IEEE Transactions on intelligent vehicles*, vol. 1, no. 1, pp. 33–55, 2016.
- [23] S. Karaman and E. Frazzoli, "Sampling-Based Algorithms for Optimal Motion Planning," *The international journal of robotics research*, vol. 30, no. 7, pp. 846–894, 2011.
- [24] L. Yang, J. Qi, J. Xiao, and X. Yong, "A Literature Review of UAV 3D Path Planning," in *Proceeding of the 11th World Congress on Intelligent Control and Automation*, pp. 2376–2381, IEEE, 2014.
- [25] M. Elbanhawi and M. Simic, "Sampling-Based Robot Motion Planning: A Review," *Ieee access*, vol. 2, pp. 56–77, 2014.
- [26] A. Richards, T. Schouwenaars, J. P. How, and E. Feron, "Spacecraft Trajectory Planning with Avoidance Constraints using Mixed-Integer Linear Programming," *Journal of Guidance, Control, and Dynamics*, vol. 25, no. 4, pp. 755–764, 2002.
- [27] A. Richards and O. Turnbull, "Inter-Sample Avoidance in Trajectory Optimizers Using Mixed-Integer Linear Programming," *International Journal of Robust and Nonlinear Control*, vol. 25, no. 4, pp. 521–526, 2015.
- [28] J. Stefan, A. R. Pedram, R. Funada, and T. Tanaka, "Rationally Inattentive Path-Planning via RRT," *arXiv preprint arXiv:2002.12494*, 2020.
- [29] P. E. Hart, N. J. Nilsson, and B. Raphael, "A Formal Basis for the Heuristic Determination of Minimum Cost Paths," *IEEE transactions on Systems Science and Cybernetics*, vol. 4, no. 2, pp. 100–107, 1968.
- [30] S. M. LaValle, *Planning Algorithms*. Cambridge university press, 2006.
- [31] T. Lipp and S. Boyd, "Variations and Extension of the Convex–Concave Procedure," *Optimization and Engineering*, vol. 17, no. 2, pp. 263–287, 2016.
- [32] J. Massey, "Causality, Feedback and Directed Information," Citeseer.
- [33] S. Tatikonda and S. Mitter, "Control under communication constraints," *IEEE Transactions on automatic control*, vol. 49, no. 7, pp. 1056–1068, 2004.
- [34] P. Giselsson and S. Boyd, "Linear Convergence and Metric Selection for Douglas-Rachford Splitting and ADMM," *IEEE Transactions on Automatic Control*, vol. 62, no. 2, pp. 532–544, 2016.
- [35] T. Goldstein, B. O’Donoghue, S. Setzer, and R. Baraniuk, "Fast Alternating Direction Optimization Methods," *SIAM Journal on Imaging Sciences*, vol. 7, no. 3, pp. 1588–1623, 2014.
- [36] J. Eckstein and D. P. Bertsekas, "On the Douglas–Rachford Splitting Method and the Proximal Point Algorithm for Maximal Monotone Operators," *Mathematical Programming*, vol. 55, no. 1–3, pp. 293–318, 1992.
- [37] R. Nishihara, L. Lessard, B. Recht, A. Packard, and M. Jordan, "A General Analysis of the Convergence of ADMM," in *International Conference on Machine Learning*, pp. 343–352, 2015.
- [38] J. Eckstein and M. C. Ferris, "Operator-splitting methods for monotone affine variational inequalities, with a parallel application to optimal control," *INFORMS Journal on Computing*, vol. 10, no. 2, pp. 218–235, 1998.
- [39] J. Eckstein, "Parallel Alternating Direction Multiplier Decomposition of Convex Programs," *Journal of Optimization Theory and Applications*, vol. 80, no. 1, pp. 39–62, 1994.
- [40] A. Lambert and D. Gruyer, "Safe Path Planning in an Uncertain-Configuration Space," in *2003 IEEE International Conference on Robotics and Automation*, vol. 3, pp. 4185–4190, IEEE, 2003.
- [41] M. ApS, "Mosek optimization suite,"